

## Channel coupling effects on the fusion excitation functions for $^{28}\text{Si} + ^{90,94}\text{Zr}$ in sub- and near-barrier regions

Sunil Kalkal,<sup>1,\*</sup> S. Mandal,<sup>1</sup> N. Madhavan,<sup>2</sup> E. Prasad,<sup>3</sup> Shashi Verma,<sup>1</sup> A. Jhingan,<sup>2</sup> Rohit Sandal,<sup>4</sup> S. Nath,<sup>2</sup> J. Gehlot,<sup>2</sup> B. R. Behera,<sup>4</sup> Mansi Saxena,<sup>1</sup> Savi Goyal,<sup>1</sup> Davinder Siwal,<sup>1</sup> Ritika Garg,<sup>1</sup> U. D. Pramanik,<sup>5</sup> Suresh Kumar,<sup>1</sup> T. Varughese,<sup>2</sup> K. S. Golda,<sup>2</sup> S. Muralithar,<sup>2</sup> A. K. Sinha,<sup>6</sup> and R. Singh<sup>1,†</sup>

<sup>1</sup>*Department of Physics and Astrophysics, University of Delhi, Delhi-110007, India*

<sup>2</sup>*Inter University Accelerator Centre, Aruna Asaf Ali Marg, New Delhi-110067, India*

<sup>3</sup>*Department of Physics, Calicut University, Calicut-673635, India*

<sup>4</sup>*Department of Physics, Panjab University, Chandigarh-160014, India*

<sup>5</sup>*Saha Institute of Nuclear Physics, 1/AF Bidhan Nagar, Kolkata-700064, India*

<sup>6</sup>*UGC-DAE CSR, Kolkata Centre, 3/LB-8, Bidhan Nagar, Kolkata-700098, India*

(Received 15 January 2010; published 21 April 2010)

Fusion excitation functions and angular distributions of evaporation residues (ERs) have been measured for  $^{28}\text{Si} + ^{90,94}\text{Zr}$  systems around the Coulomb barrier using the recoil mass spectrometer, Heavy Ion Reaction Analyzer (HIRA). For both systems, the experimental fusion cross sections are strongly enhanced compared to the predictions of the one-dimensional barrier penetration model (1-d BPM) below the barrier. Coupled channels formalism has been employed to theoretically explain the observed sub-barrier fusion cross section enhancement. The enhancement could be explained by considering the coupling of the low-lying inelastic states of the projectile and target in the  $^{28}\text{Si} + ^{90}\text{Zr}$  system. In the sub-barrier region, the measured fusion cross sections for  $^{28}\text{Si} + ^{94}\text{Zr}$  turned out to be about an order of magnitude higher than the ones for the  $^{28}\text{Si} + ^{90}\text{Zr}$  system, which could not be explained by coupling to inelastic states alone. This observation indicates the importance of multinucleon transfer reaction channels with positive  $Q$  values in the sub-barrier fusion cross section enhancement, because  $^{90,94}\text{Zr}$  are believed to have similar collective strengths. This implies that no strong isotopic dependence of fusion cross sections is expected as far as the couplings to collective inelastic states are concerned. In addition, the role of projectile and multiphonon couplings in the enhancement has been explored.

DOI: [10.1103/PhysRevC.81.044610](https://doi.org/10.1103/PhysRevC.81.044610)

PACS number(s): 25.70.Jj, 25.70.Hi

### I. INTRODUCTION

Understanding the dynamics of heavy ion fusion reactions and the interplay of nuclear structure and nuclear reactions has been a subject of intensive study during the last few decades [1–3]. Quite a large enhancement in the sub-barrier heavy ion fusion cross sections (one to two orders of magnitude) over the prediction of 1-d BPM has been observed experimentally [1–14]. This enhancement could be explained in terms of the coupling of relative motion to internal degrees of freedom of the colliding nuclei associated with specific details of the colliding partners such as deformation [4–6], vibration [7–10], and nucleon transfer channels [11–14] or related to the gross features of nuclear matter such as neck formation [15,16] between the two colliding nuclei. The role of static deformations and collective surface vibrations has been unambiguously established, but the precise effect of transfer channels has been seemingly elusive in most cases. The inelastic part can be coupled easily, but for the transfer part, with an increasing number of nucleons getting transferred, more and more channels open up, making coupling very complicated. To disentangle the role of transfer channels from that of collective excitations in enhancement, systems are

generally selected in which one target isotope has a closed shell or closed sub-shell and the other one has some nucleons outside the closed shell (so that there are some positive  $Q$ -value transfer channels). In addition, if both of the target nuclei have similar collective strengths, then the experimental signature of transfer couplings becomes noticeable while comparing two systems.

The systems which have been extensively studied to see the role of transfer channels in the sub-barrier region are  $^{40}\text{Ca} + ^{90,96}\text{Zr}$  [17–19], where a strong interplay of collectivity and transfer in fusion enhancement has been observed. But very soon it was realized that  $^{96}\text{Zr}$  is a stronger octupole vibrator than  $^{90}\text{Zr}$ ; the observed enhancement may be due to that difference rather than to the transfer channels' playing a major role. To verify this, experiments with  $^{36}\text{S}, ^{48}\text{Ca} + ^{90,96}\text{Zr}$  systems [20,21] were performed. For all cases, the transfer channels have large negative  $Q$  values. In a more recent experiment, fusion cross sections of  $^{40}\text{Ca} + ^{94}\text{Zr}$  were measured [22] in which up to six neutron pickup channels have positive  $Q$  values. When these cross sections were plotted on a reduced scale, it was found that there was something special about the  $^{40}\text{Ca} + ^{96}\text{Zr}$  system which could be associated with the multinucleon transfer channels; the  $^{40,48}\text{Ca} + ^{90}\text{Zr}$  systems have very similar fusion cross sections, and  $^{48}\text{Ca} + ^{96}\text{Zr}$  sub-barrier fusion cross sections were almost a factor of 10 higher, which could be attributed to the coupling of octupole vibrations of the target nucleus. The  $^{40}\text{Ca} + ^{94,96}\text{Zr}$  fusion cross sections were still higher by up to two orders of magnitude than those

\*kalkal84@gmail.com

†Present address: AINST, Amity University, Noida, India.

of  $^{40,48}\text{Ca} + ^{90}\text{Zr}$  at the lowest energies [22]. This investigation indicates that the involved fusion reaction dynamics is much more complicated than simple inclusion of couplings to vibrational states of fusing nuclei and one or two nucleon transfer channels.

In the present paper, we report the measurement of fusion excitation functions for  $^{28}\text{Si} + ^{90,94}\text{Zr}$  systems. The aim of this experiment was to extricate the role of multinucleon transfer channels from inelastic excitations, as both isotopes have similar quadrupole and octupole strengths, and to investigate the role of the projectile shape and deformation strength in the sub-barrier fusion cross section enhancement. For the  $^{90}\text{Zr}$  target, fusion excitation function measurements have already been performed using  $^{33}\text{S}$  [23] and  $^{46}\text{Ti}$  [24] (prolate shaped);  $^{36}\text{S}$  [20],  $^{50}\text{Ti}$  [24], and  $^{58}\text{Ni}$  [25] (neutron or proton magic); and  $^{40}\text{Ca}$  [19] and  $^{48}\text{Ca}$  [21] (doubly magic) projectiles. Therefore, an oblate-shaped  $^{28}\text{Si}$  nucleus [26] was chosen. Moreover, for  $^{90,94}\text{Zr}$ , with  $Z = 40$  sub-shell closure, proton transfer channels are not expected to play any significant role.  $^{90}\text{Zr}$  is a neutron magic nucleus with the expectation of suppression of neutron pickup channels owing to the corresponding negative  $Q$  values. The  $^{28}\text{Si} + ^{92}\text{Zr}$  system, on which fusion data already exist in the literature [9], has only one transfer channel ( $2n$  pickup) with a positive  $Q$  value. In the case of  $^{94}\text{Zr}$ , there are four neutrons outside the closed shell, and up to four neutron pickup channels have positive  $Q$  values. Therefore, it should be possible to clearly observe the effect of single as well as multineutron transfer channels in the sub-barrier fusion cross section enhancement by comparing these systems.

## II. EXPERIMENTAL DETAILS

The experiment was carried out using a pulsed  $^{28}\text{Si}$  beam (2  $\mu\text{s}$  repetition rate) from the 15UD Pelletron accelerator at the Inter University Accelerator Centre (IUAC), New Delhi. The  $^{90,94}\text{Zr}$  targets (having respective enrichments of 97.65% and 96.07%), each with a thickness of 280  $\mu\text{g}/\text{cm}^2$  on 45  $\mu\text{g}/\text{cm}^2$  carbon backings, were used [27]. Fusion excitation function measurements were carried out using the recoil mass spectrometer, the Heavy Ion Reaction Analyzer (HIRA) [28], at laboratory energies ( $E_{\text{lab}}$ ) from 82 to 120 MeV in steps of 2 MeV near the barrier and 3–5 MeV above the barrier, covering a range from  $\sim 13\%$  below to  $\sim 27\%$  above the Coulomb barrier. In the sliding seal target chamber of HIRA, two silicon surface barrier detectors were mounted at angles of  $\pm 25^\circ$  with respect to beam direction for normalization to obtain the evaporation residue (ER) cross section and for beam monitoring. A carbon charge reset foil of 35  $\mu\text{g}/\text{cm}^2$  thickness was used 10 cm downstream of the target for charge reequilibration of ERs which may be shifted by an internal conversion process. The ERs were dispersed at the focal plane of the HIRA according to their  $m/q$  values. At the focal plane of the HIRA, a position-sensitive multiwire proportional counter (MWPC) with an active area of  $150 \times 50 \text{ mm}^2$  was used. For performing the fusion excitation function measurements, HIRA was kept at  $0^\circ$  with respect to the beam direction with 5 mSr ( $\pm 2.28^\circ$ ) solid angle acceptance. For measuring angular distributions of ERs, the HIRA solid angle was changed to 1 mSr, and measurements were done in steps of

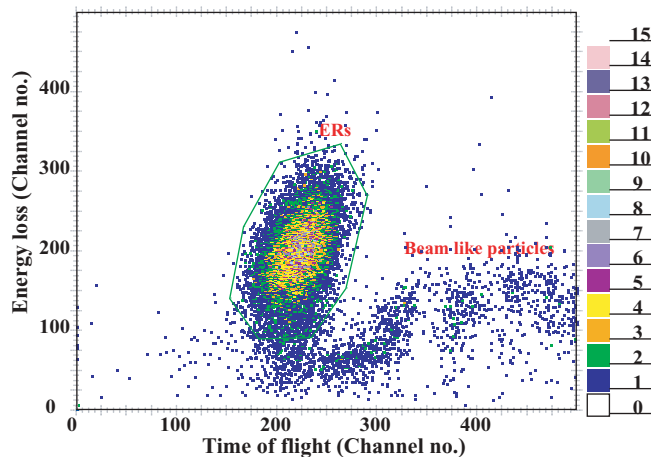


FIG. 1. (Color online) Two-dimensional spectrum showing the energy loss of particles in MWPC vs TOF for  $^{28}\text{Si} + ^{94}\text{Zr}$  system at 103 MeV ( $E_{\text{lab}}$ ). Both  $x$  and  $y$  axes are given in channel numbers.

$2^\circ$  from  $0^\circ$  to  $10^\circ$ , at 103 MeV ( $E_{\text{lab}}$ ) for  $^{28}\text{Si} + ^{90,94}\text{Zr}$  systems by rotating HIRA about the beam axis. The timing information in the form of time of flight (TOF) was obtained through a time to amplitude converter with the arrival of particles at the focal plane (MWPC) as the start signal and delayed rf as the stop signal. This TOF was very helpful in separating multiply scattered beamlike particles reaching the focal plane from ERs, as shown in Fig. 1. Excellent primary beam rejection and clean separation between beamlike particles and ERs enabled us to measure cross sections down to a few microbarns. At 120 MeV ( $E_{\text{lab}}$ ), HIRA was scanned for charge states, mass, and energy of ERs for both the systems [13,14]. For other incident energies, the HIRA fields were scaled appropriately.

In the fusion excitation functions, the ER cross section was taken to be the fusion cross section, because the fission was negligible for these systems. The ER cross sections were calculated using the expression

$$\sigma_{\text{fus}} = \frac{1}{\eta} \left( \frac{Y_{\text{ER}}}{Y_M} \right) \left( \frac{d\sigma}{d\Omega} \right)_R \Omega_M,$$

where  $\eta$  is the average HIRA efficiency for ER detection,  $Y_{\text{ER}}$  is the yield of ERs,  $Y_M$  is the geometric mean of the monitor yields,  $(d\sigma/d\Omega)_R$  is the Rutherford cross section in the laboratory, and  $\Omega_M$  is the solid angle subtended by the monitors at the target.

The HIRA transmission efficiency was measured by the coincident  $\gamma$ -ray method for  $^{28}\text{Si} + ^{94}\text{Zr}$  at 103 MeV ( $E_{\text{lab}}$ ). A singles  $\gamma$ -ray spectrum was taken, and then during offline analysis, the TOF gate was put to get  $\gamma$ 's which were in coincidence with the particles reaching the focal plane. The ratio of counts for a specific  $\gamma$  in the coincidence spectrum ( $N_{\text{coin}}$ ) to those in the singles ( $N_{\text{singles}}$ ) spectrum gave the HIRA transmission efficiency for this system. For the identified  $\gamma$  line (675.2 keV), the HIRA efficiency so obtained was 3.2%. Figure 2 shows coincidence as well as singles  $\gamma$  spectra. Detection efficiency of ERs depends on the distributions of charge, mass, energy, and angle of the particles entering HIRA and on the charge, mass, angular, and energy acceptance of

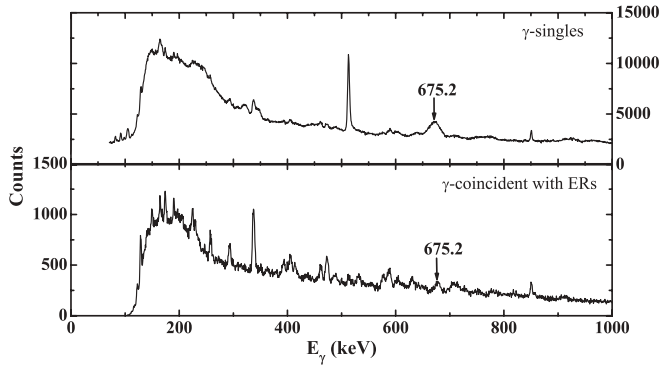


FIG. 2.  $\gamma$ -ray spectra: Singles spectrum (above) and coincidence (with ERs) spectrum (below).

HIRA. The distributions are reaction dependent, while the physical acceptances are the same for all the systems. Absolute detection efficiency for various ERs at all beam energies was calculated by a combination of theoretical estimates of the charge state distribution (by using Sayer's empirical formula [29]), energy and angular distribution of ERs (by using PACE3 [30]), and mass related efficiency (experimentally measured) as

$$\eta_{\text{HIRA}} = \eta_q \eta_E \eta_\theta \eta_m.$$

The efficiency so calculated was found to be in very good agreement with that obtained by the  $\gamma$ -ray method, and this method of HIRA efficiency calculation has been adopted in estimating the fusion cross sections. As the ERs were not very far in mass for  $^{28}\text{Si} + ^{90}\text{Zr}$ , similar values were used after checking with the simulation program. Theoretical calculations were also performed using the Monte Carlo simulation code TERS [31], and the efficiency obtained by simulation agreed reasonably well with the efficiency obtained experimentally and calculated by PACE3, as given in Table I.

### III. RESULTS AND DISCUSSION

The measured fusion cross sections for  $^{28}\text{Si} + ^{90,94}\text{Zr}$  systems are listed in Table II. Corrections for loss of beam energy in carbon backing and half target thickness were taken into account. Data for the  $^{28}\text{Si} + ^{92}\text{Zr}$  system used in this section are taken from Ref. [9]. In the present data, the errors are absolute errors consisting of the statistical error and error in the HIRA transmission efficiency. For the  $^{28}\text{Si} + ^{92}\text{Zr}$  system, only statistical error was taken into account. Coupled-channels formalism CCFULL [32] was employed to analyze the data. Various types of potentials had been proposed to explain

TABLE I. HIRA transmission efficiency of ERs for  $^{28}\text{Si} + ^{94}\text{Zr}$  system at 103 MeV ( $E_{\text{lab}}$ ).

ER	$E_\gamma$ (keV)	Expt. (%)	PACE3 (%)	TERS (%) (simulation)
$^{118}\text{I}$ (41%)	675.6	$3.2 \pm 0.08$	3.67	3.01
$^{119}\text{I}$ (15%)	674.6		2.90	2.36

TABLE II. Fusion cross sections ( $\sigma_{\text{fus}}$ ) and errors in cross sections ( $\delta\sigma$ ) at center-of-mass energies ( $E_{\text{c.m.}}$ ) for  $^{28}\text{Si} + ^{90,94}\text{Zr}$  systems.

$E_{\text{c.m.}}$ (MeV)	$\sigma_{\text{fus}}$ (mb)	$\delta\sigma$ (mb)
<b><math>^{28}\text{Si} + ^{90}\text{Zr}</math></b>		
65.7	0.049	0.009
67.3	0.435	0.058
68.9	2.317	0.287
70.4	9.770	1.19
72.0	42.60	5.19
73.6	81.18	9.79
75.2	129.2	15.5
76.7	169.1	20.6
79.1	251.5	31.7
82.2	450.3	85.1
84.6	599.0	110.8
88.5	680.1	125.0
92.4	674.3	126.4
<b><math>^{28}\text{Si} + ^{94}\text{Zr}</math></b>		
63.3	0.037	0.006
65.0	0.201	0.029
66.6	2.160	0.310
68.2	10.70	1.48
69.7	26.57	3.68
71.3	52.04	7.28
72.9	100.2	13.9
74.5	138.8	19.3
76.1	165.4	23.1
77.7	216.0	29.6
80.0	285.6	41.1
83.2	467.7	87.9
85.6	565.0	126.4
89.6	599.2	110.0
93.5	542.0	98.2

fusion data over different energy ranges [33–35]. The ion-ion potentials used in these calculations were Woods-Saxon parametrization of the Akyuz-Winther (AW) [36] potential. Potential parameters so calculated are listed in Table III. These potential parameters have been used without any attempt to vary them to fit the above barrier data. The deformation parameters associated with the transition of multipolarity  $\lambda$  were calculated from measured transition probabilities  $B(E2)$  [37] and  $B(E3)$  [38] using the expression

$$\beta_\lambda = \frac{4\pi}{3ZR^\lambda} \sqrt{\left[ \frac{B(E\lambda) \uparrow}{e^2} \right]}.$$

TABLE III. Parameters of AW potential (Woods-Saxon form) used in coupled-channels calculations for all the systems.

System	$V_0$ (MeV)	$r_0$ (fm)	$a$ (fm)
$^{28}\text{Si} + ^{90}\text{Zr}$	66.01	1.176	0.659
$^{28}\text{Si} + ^{92}\text{Zr}$	66.25	1.176	0.660
$^{28}\text{Si} + ^{94}\text{Zr}$	66.49	1.176	0.660

TABLE IV. Deformation parameters and excitation energies along with the spins and parities of the states of the nuclei used in the coupled-channels calculations.

Nucleus	$J^\pi$	$E_x$ (MeV)	$\beta$
$^{90}\text{Zr}$	$2^+$	2.19	0.089
	$3^-$	2.75	0.211
$^{92}\text{Zr}$	$2^+$	0.93	0.103
	$3^-$	2.34	0.174
$^{94}\text{Zr}$	$2^+$	0.92	0.090
	$3^-$	2.06	0.193
$^{28}\text{Si}$	$2^+$	1.78	-0.407
	$3^-$	6.88	0.280

Here  $R$  is radius ( $R = r_c A^{1/3}$ ) of the nucleus which is excited, and  $r_c$  is taken to be 1.2 fm. The values of  $\beta_\lambda$  so calculated along with the excitation energies of the involved nuclei are given in Table IV.

In Fig. 3, measured cross sections for  $^{28}\text{Si} + ^{90}\text{Zr}$  are shown along with the theoretical calculations using CCFULL. The sub-barrier fusion cross sections estimated by 1-d BPM are an order of magnitude smaller than the experimentally measured cross sections. Coupled-channels calculations were performed for this system including  $2^+$ ,  $3^-$  states of the target one after the other, and it was found that the  $3^-$  state enhances the cross sections more than the  $2^+$  state of the target, implying that coupling to the  $3^-$  state is stronger in this case. Inclusion of  $0^+$ ,  $2^+$  states of  $^{28}\text{Si}$  further increases the sub-barrier fusion cross section. However, if the  $4^+$  state of the projectile is also included, then it over predicts the fusion cross section near as well as below the barrier, as shown in Fig. 3(a). A large part of the increase in calculated cross sections is contributed by the strong projectile inelastic excitation. As the  $2^-$  state of  $^{28}\text{Si}$  is significantly high in energy (6.878 MeV), it is not expected to play any major role [39]. CCFULL calculations were also performed assuming  $^{28}\text{Si}$  as a vibrator, taking  $2^+$  as a phonon state. But that did not reproduce the data well. It was found that calculations including two-phonon states of the octupole mode [ $2^+$ ,  $3^-$ ,  $2^+ \otimes 3^-$ ,  $(3^-)^2$ ,  $2^+ \otimes (3^-)^2$ ] in  $^{90}\text{Zr}$  and  $0^+$ ,  $2^+$  states of  $^{28}\text{Si}$ , reproduced the data reasonably well, as shown in Fig. 3(b). Mutual target and projectile excitations were taken into consideration while performing these calculations. In this case, further inclusion of multiphonon couplings was found to have insignificant effect on the cross sections. The transfer reaction cross sections for the  $^{28}\text{Si} + ^{90}\text{Zr}$  system are expected to be small and, therefore, their influence on the sub-barrier fusion cross section enhancement will be negligible. Though the  $\alpha$  pickup channel has a small positive  $Q$  value, this channel does not seem to make any significant contribution to the sub-barrier fusion cross section enhancement.

Using a similar coupling scheme as for  $^{28}\text{Si} + ^{90}\text{Zr}$ , coupled-channels calculations were performed for the  $^{28}\text{Si} + ^{92}\text{Zr}$  system for which fusion cross section data already exist [9]. These calculations along with experimental data points are shown in Fig. 4. It was found that apart from the inclusion of inelastic couplings, one has to take into account the transfer channel to reproduce the data better. For this system,

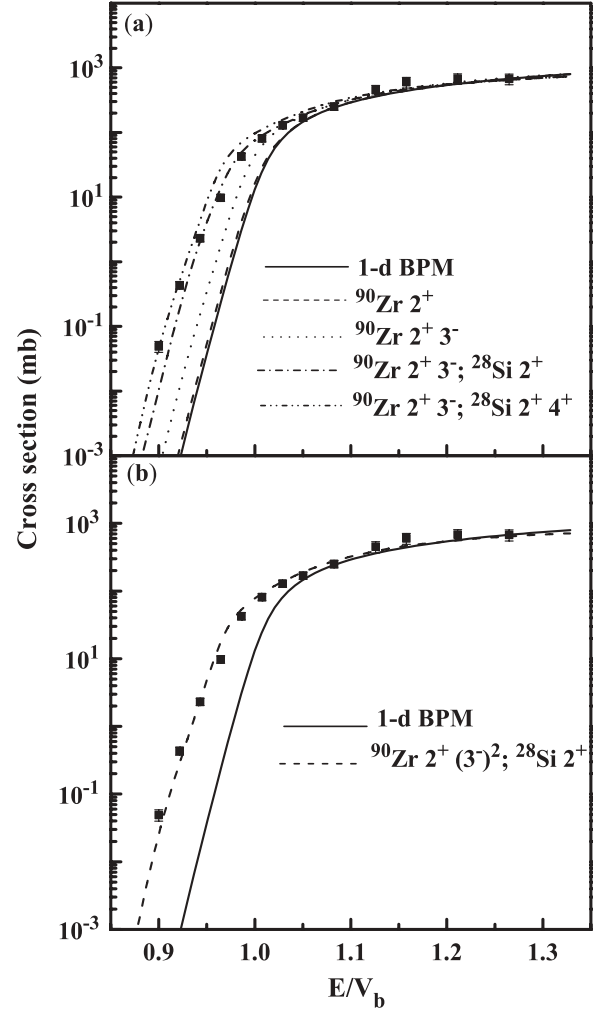


FIG. 3.  $^{28}\text{Si} + ^{90}\text{Zr}$  fusion excitation function along with the theoretical calculations using CCFULL. The results of exact coupled-channels calculations including various vibrational states of the target and rotational states of  $^{28}\text{Si}$  along with the 1-d BPM calculations.

the two-neutron pickup channel has a positive  $Q$  value (see Table V). The strength of the form factor for two-particle transfer in CCFULL was varied to explain the experimental data (with equivalent  $\beta = 0.30$ ).

Fusion data of the  $^{28}\text{Si} + ^{94}\text{Zr}$  system were analyzed by including several inelastic channels one by one. For this system also, coupling to inelastic excitations predicted cross sections in the sub-barrier region that were much smaller than the experimental values. Even inclusion of two-neutron pickup was not able to reproduce the experimental cross sections, though it enhanced the sub-barrier cross sections to some extent, as shown in Fig. 5. In this case, up to four neutron pickup channels have positive  $Q$  values as given in Table V. It is clear that one needs to include more transfer channels in this case. Since CCFULL provides the option of including just one pair transfer channel and treats it in too simple a way, it is not possible to unambiguously infer the role of transfer channels in the observed enhancement. One needs to perform full coupled-channels calculations including all the transfer channels appropriately. However, it is observed that

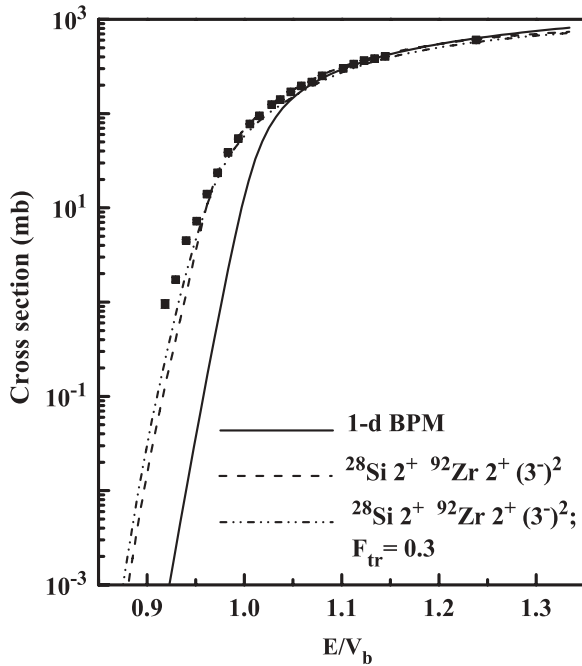


FIG. 4.  $^{28}\text{Si} + ^{92}\text{Zr}$  fusion excitation function along with the theoretical calculations using CCFULL. The results of exact coupled-channels calculations including various inelastic states of target as well as projectile and two-neutron pickup transfer channel along with the 1-d BPM calculations.

the inelastic couplings enhance the sub-barrier fusion cross sections significantly and that by almost a similar amount for each target, implying the similarity of low-lying states of the  $^{90,94}\text{Zr}$  isotopes.

In Fig. 6, a comparative cross section plot for all the systems in the sub- and near-barrier region is shown on a reduced scale. One can see a significant enhancement in the sub-barrier fusion cross sections for  $^{28}\text{Si} + ^{92,94}\text{Zr}$  as compared to the  $^{28}\text{Si} + ^{90}\text{Zr}$  system, clearly providing evidence of the role of neutron transfer channels in enhancement. Almost an order of magnitude enhancement is observed in  $^{28}\text{Si} + ^{94}\text{Zr}$  as compared to  $^{28}\text{Si} + ^{92}\text{Zr}$ , giving clear evidence of the role of multinucleon transfer channels in fusion cross section enhancement. As it is, one-neutron transfer might be the most dominant channel, because it has the largest cross section among all transfer channels. However, from the results reported here, it is clear that even the multinucleon transfer channels play a significant role in the enhancement of sub-barrier fusion cross sections.

To explore the role of projectile deformation in the enhancement, fusion cross sections of various projectiles with

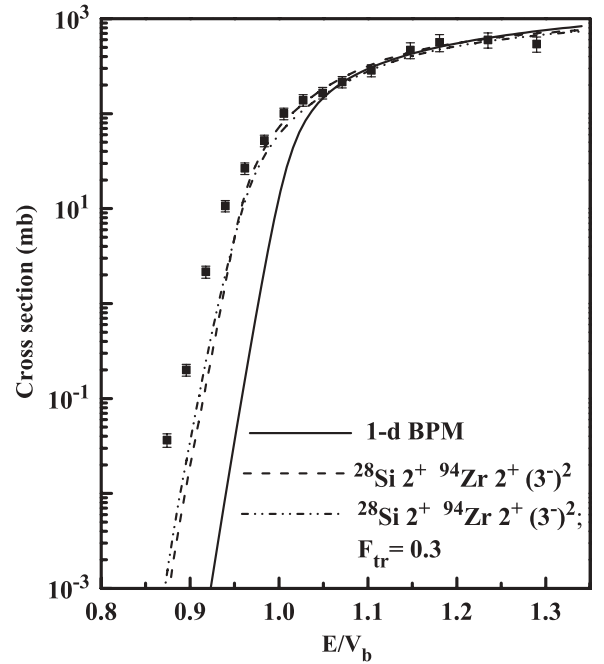


FIG. 5.  $^{28}\text{Si} + ^{94}\text{Zr}$  fusion excitation function along with the theoretical calculations using CCFULL. The results of exact coupled-channels calculations including various inelastic states of target as well as projectile and two-neutron pickup transfer channel along with the 1-d BPM calculations.

a  $^{90}\text{Zr}$  target are shown in Fig. 7. When fusion cross sections for all systems divided by the square of the barrier radius were plotted against energy divided by the barrier height, it was found that the results of 1-d BPM calculations were quite different for each system in the sub-barrier region. Therefore, Wong's expression

$$\sigma_{\text{fus}} = \frac{R_b^2 \hbar \omega}{2E_{\text{c.m.}}} \ln \left[ 1 + \exp \left( 2\pi \frac{E_{\text{c.m.}} - V_b}{\hbar \omega} \right) \right],$$

where  $R_b$  is the barrier radius,  $\hbar \omega$  is a measure of barrier curvature,  $V_b$  is the barrier height,  $E_{\text{c.m.}}$  is the energy in the center-of-mass frame, was used. The  $\sigma_{\text{red}}$  and  $E_{\text{red}}$  were defined as

$$\sigma_{\text{red}} = 2\sigma_{\text{fus}} E_{\text{c.m.}} / R_b^2 \hbar \omega,$$

$$E_{\text{red}} = (E_{\text{c.m.}} - V_b) / \hbar \omega.$$

To match the results of 1-d BPM,  $\sigma_{\text{red}}$  vs  $E_{\text{red}}$  were plotted for all the systems in the entire energy range. The values of  $V_b$ ,  $\hbar \omega$ , and  $R_b$  were obtained by using AW potential parameters in CCFULL calculations. One more thing to be noted is that in all the cases shown in Fig. 7, most of the transfer channels

TABLE V. Ground-state  $Q$  values (in MeV) for various transfer channels for  $^{28}\text{Si} + ^{90,92,94}\text{Zr}$  systems.  $n$ ,  $p$ , and  $\alpha$  denote neutron, proton, and  $\alpha$  transfer channels, respectively.

System	+1n	+2n	+3n	+4n	+1p	-1p	-1n	-\alpha	+\alpha
$^{28}\text{Si} + ^{90}\text{Zr}$	-3.50	-2.20	-7.96	-8.37	-5.60	-6.43	-9.98	-7.92	0.28
$^{28}\text{Si} + ^{92}\text{Zr}$	-0.16	3.25	-2.13	-2.24	-6.65	-5.54	-10.44	-7.22	3.99
$^{28}\text{Si} + ^{94}\text{Zr}$	0.25	4.13	2.08	4.09	-7.58	-4.78	-10.72	-6.71	3.20

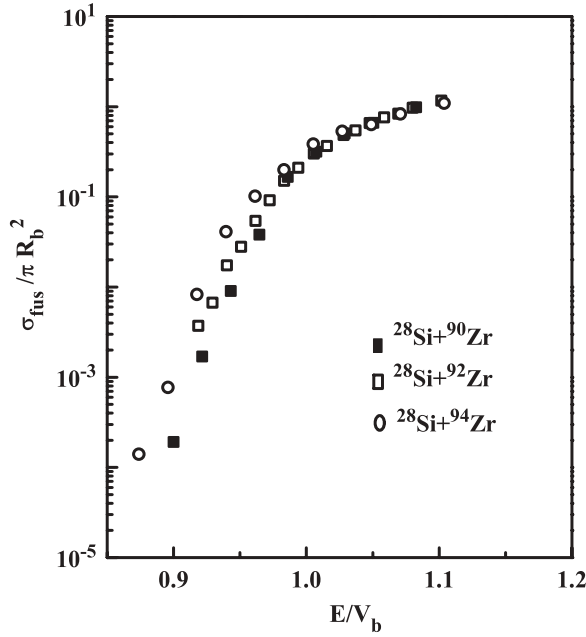


FIG. 6. Experimental fusion excitation functions for  $^{28}\text{Si} + ^{90,92,94}\text{Zr}$  on a reduced scale (see text).

have negative  $Q$  values. Hence, transfer channels will play an insignificant role in enhancing the sub-barrier fusion cross sections for these systems. Out of these projectiles,  $^{40,48}\text{Ca}$  are doubly magic,  $^{58}\text{Ni}$  is proton magic, and  $^{50}\text{Ti}$  and  $^{36}\text{S}$  are neutron magic, whereas  $^{28}\text{Si}$ ,  $^{33}\text{S}$ , and  $^{46}\text{Ti}$  are midshell nuclei. Among the midshell nuclei,  $^{28}\text{Si}$  is oblate deformed ( $\beta_2 = -0.407$ ), whereas  $^{33}\text{S}$  ( $\beta_2 = 0.282$ ) and  $^{46}\text{Ti}$  ( $\beta_2 = 0.317$ ) are prolate-deformed nuclei. The deformation parameter for  $^{33}\text{S}$  is

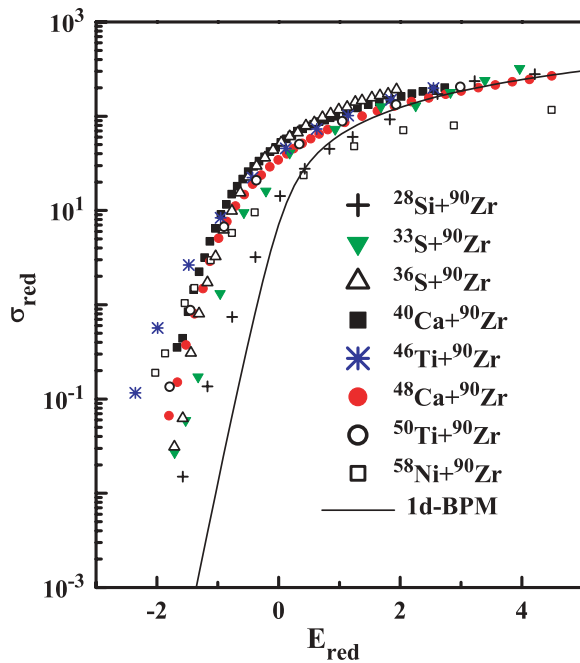


FIG. 7. (Color online) Fusion excitation functions for  $^{28}\text{Si}$ ,  $^{33,36}\text{S}$ ,  $^{40,48}\text{Ca}$ ,  $^{46,50}\text{Ti}$ , and  $^{58}\text{Ni} + ^{90}\text{Zr}$  systems on a reduced scale to match the 1-d BPM values (see the text).  $E_{\text{red}}$  and  $\sigma_{\text{red}}$  are unitless quantities.

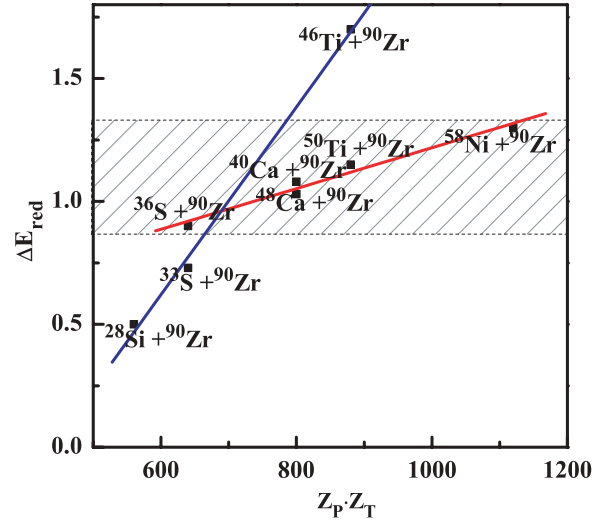


FIG. 8. (Color online)  $\Delta E_{\text{red}}$  vs product of atomic numbers of the colliding nuclei.  $\Delta E_{\text{red}}$  is the difference between the values of  $E_{\text{red}}$  corresponding to the cross sections (at 0.1 mb level) for various systems and those of  $E_{\text{red}}$  corresponding to 0.1 mb fusion cross section as obtained by 1-d BPM calculations (see Fig. 7 and the text). Systems in the hatched area are the ones with closed-shell projectiles (proton, neutron, or both closed shells).

taken as the average of  $^{32}\text{S}$  and  $^{34}\text{S}$ . It can be clearly seen from Fig. 7 that the reduced excitation functions involving doubly magic nuclei and magic nuclei (proton or neutron) have the same slopes. In the case of  $^{58}\text{Ni} + ^{90}\text{Zr}$ , the experimental data points are lower than the predictions of 1-d BPM. This was found to be so in the original paper too [25]. All the midshell nuclei have different slopes.

In Fig. 8,  $\Delta E_{\text{red}}$ , the difference in the values of  $E_{\text{red}}$  corresponding to the experimental cross sections (at 0.1 mb level) for various systems and those of  $E_{\text{red}}$  corresponding to 0.1 mb fusion cross section as obtained by 1-d BPM calculations, vs the product of the atomic numbers of colliding nuclei are plotted. It can be seen that all the systems with magic and doubly magic projectiles have a different slope as compared to the systems with midshell projectiles. For midshell projectiles, the slope is much steeper than for the magic or doubly magic projectiles, implying that the observed enhancement in the sub-barrier fusion cross section increases rapidly with the product of atomic numbers of colliding nuclei for systems with deformed projectiles. For the  $^{28}\text{Si} + ^{90}\text{Zr}$  system, the difference is minimum, contradictory to expectations if it is a highly deformed oblate nucleus and if the projectile plays a major role in the sub-barrier fusion cross section enhancement.

#### IV. SUMMARY

Fusion excitation functions were measured for the  $^{28}\text{Si} + ^{90,94}\text{Zr}$  systems to explore the role of multinucleon transfer channels and projectile deformation in the sub-barrier fusion cross section enhancement. Both the targets have similar quadrupole and octupole strengths. The angular distributions of ERs and the transmission efficiency of the HIRA were

also measured at 103 MeV ( $E_{\text{lab}}$ ). It was found that for  $^{28}\text{Si} + ^{90,94}\text{Zr}$  systems, AW potential parameters were able to reproduce the data reasonably well at all energies. Reasonable fits to the fusion excitation functions for  $^{28}\text{Si} + ^{90}\text{Zr}$  were obtained by coupling to various inelastic states of the projectile and target. Mutual excitations between target and projectile were also taken into account. It was found that taking  $^{28}\text{Si}$  as an oblate-deformed nucleus could explain the data reasonably well rather than taking it as a vibrator. The role of multiphonon couplings was also probed for these systems and was found to be of little significance. The  $^{28}\text{Si} + ^{92}\text{Zr}$  data, which were already available in the literature, were analyzed using a similar inelastic coupling scheme. It was found that these data were better reproduced by including a two-neutron pickup channel. As far as the  $^{28}\text{Si} + ^{94}\text{Zr}$  system is concerned, even inclusion of the two-nucleon transfer channel was not able to explain the data, and in fact a large enhancement remained unexplained. It seems as if multinucleon transfer channels are playing a major role in the observed enhancement for this system. A comparison between  $^{28}\text{Si} + ^{92}\text{Zr}$  and  $^{28}\text{Si} + ^{94}\text{Zr}$  systems gives a clear indication

of the importance of multineutron pickup channels in the observed enhancement. Independent of CCFULL calculations, the trend of the data supports the fact that multinucleon transfer channels with positive  $Q$  values play an important role in the sub-barrier fusion cross section enhancement. CCFULL does not handle transfer channels couplings properly, and one can include only one pair transfer channel with a form factor. It was also observed that enhancement in the sub-barrier fusion cross sections increases more rapidly with the product of atomic numbers of colliding nuclei for midshell projectiles as compared to closed-shell projectiles.

### ACKNOWLEDGMENTS

We are thankful to the Pelletron staff of IUAC for providing a stable beam. We are indebted to the target laboratory staff, especially Mr. S. R. Abhilash, for help in the preparation of good quality isotopic targets. Sunil Kalkal gratefully acknowledges a research grant from CSIR, New Delhi.

- 
- [1] M. Dasgupta, D. J. Hinde, N. Rowley, and A. M. Stefanini, *Annu. Rev. Nucl. Part. Sci.* **48**, 401 (1998).
- [2] S. G. Steadman and M. J. Rhoades-Brown, *Annu. Rev. Nucl. Part. Sci.* **36**, 649 (1986).
- [3] M. Beckerman, *Rep. Prog. Phys.* **51**, 1047 (1988).
- [4] J. R. Leigh *et al.*, *Phys. Rev. C* **52**, 3151 (1995).
- [5] J. D. Bierman, P. Chan, J. F. Liang, M. P. Kelly, A. A. Sonzogni, and R. Vandenbosch, *Phys. Rev. Lett.* **76**, 1587 (1996).
- [6] R. G. Stokstad and E. E. Gross, *Phys. Rev. C* **23**, 281 (1981).
- [7] A. M. Stefanini, G. Fortuna, A. Tivelli, W. Meczynski, S. Beghini, C. Signorini, S. Lunardi, and M. Morando, *Phys. Rev. C* **30**, 2088 (1984).
- [8] A. M. Stefanini, D. Ackermann, L. Corradi, J. H. He, G. Montagnoli, S. Beghini, F. Scarlassara, and G. F. Segato, *Phys. Rev. C* **52**, R1727 (1995).
- [9] J. O. Newton, C. R. Morton, M. Dasgupta, J. R. Leigh, J. C. Mein, D. J. Hinde, H. Timmers, and K. Hagino, *Phys. Rev. C* **64**, 064608 (2001).
- [10] A. M. Stefanini *et al.*, *Phys. Rev. Lett.* **74**, 864 (1995).
- [11] V. I. Zagrebaev, *Phys. Rev. C* **67**, 061601 (2003).
- [12] V. Yu. Denisov, *Eur. Phys. J. A* **7**, 87 (2000).
- [13] Vandana Tripathi *et al.*, *Phys. Rev. C* **65**, 014614 (2001).
- [14] Lagy T. Baby *et al.*, *Phys. Rev. C* **56**, 1936 (1997).
- [15] C. E. Aguiar, V. C. Barbosa, L. F. Canto, and R. Donangelo, *Nucl. Phys. A* **472**, 571 (1987).
- [16] C. E. Aguiar, L. F. Canto, and R. Donangelo, *Phys. Rev. C* **31**, 1969 (1985).
- [17] Ning Wang, Xizhen Wu, and Zhuxia Li, *Phys. Rev. C* **67**, 024604 (2003).
- [18] G. Montagnoli, S. Beghini, F. Scarlassara, A. M. Stefanini, L. Corradi, C. J. Lin, G. Pollarolo, and Aage Winther, *Eur. Phys. J. A* **15**, 351 (2002).
- [19] H. Timmers, L. Corradi, A. M. Stefanini, D. Ackermann, J. H. He, S. Beghini, G. Montagnoli, F. Scarlassara, G. F. Segato, and N. Rowley, *Phys. Lett. B* **399**, 35 (1997).
- [20] A. M. Stefanini, L. Corradi, A. M. Vinodkumar, Yang Feng, F. Scarlassara, G. Montagnoli, S. Beghini, and M. Bisogno, *Phys. Rev. C* **62**, 014601 (2000).
- [21] A. M. Stefanini *et al.*, *Phys. Rev. C* **73**, 034606 (2006).
- [22] A. M. Stefanini *et al.*, *Phys. Rev. C* **76**, 014610 (2007).
- [23] L. Corradi *et al.*, *Z. Phys. A* **334**, 55 (1990).
- [24] P. H. Stelson, H. J. Kim, M. Beckerman, D. Shapira, and R. L. Robinson, *Phys. Rev. C* **41**, 1584 (1990).
- [25] F. Scarlassara, S. Beghini, F. Soramel, C. Signorini, L. Corradi, G. Montagnoli, D. R. Napoli, A. M. Stefanini, and Zhi-Chang Li, *Z. Phys. A* **338**, 171 (1991).
- [26] R. H. Spear, *Phys. Rep.* **73**, 369 (1981).
- [27] Sunil Kalkal, S. R. Abhilash, D. Kabiraj, S. Mandal, N. Madhavan, and R. Singh, *Nucl. Instrum. Methods Phys. Res. A* **613**, 190 (2010).
- [28] A. K. Sinha, N. Madhavan, J. J. Das, P. Sugathan, D. O. Kataria, A. P. Patro, and G. K. Mehta, *Nucl. Instrum. Methods Phys. Res. A* **339**, 543 (1994).
- [29] R. O. Sayer, *Rev. Phys. Appl. (Paris)* **12**, 1543 (1977).
- [30] A. Gavron, *Phys. Rev. C* **21**, 230 (1980).
- [31] S. Nath, *Comput. Phys. Commun.* **179**, 492 (2008).
- [32] K. Hagino, N. Rowley, and A. T. Kruppa, *Comput. Phys. Commun.* **123**, 143 (1999).
- [33] G. P. A. Nobre, L. C. Chamon, L. R. Gasques, B. V. Carlson, and I. J. Thompson, *Phys. Rev. C* **75**, 044606 (2007).
- [34] K. Siwek-Wilczynska and J. Wilczynski, *Phys. Rev. C* **64**, 024611 (2001).
- [35] A. B. Balantekin and S. Kuyucak, *J. Phys. G* **23**, 1159 (1997).
- [36] R. A. Broglia and A. Winther, *Heavy Ion Reaction Lecture Notes, Vol. 1: Elastic and Inelastic Reactions* (Benjamin/Cummings, Reading, MA, 1981).
- [37] S. Raman, C. W. Nestor Jr., and P. Tikkanen, *At. Data Nucl. Data Tables* **78**, 1 (2001).
- [38] T. Kibedi and R. H. Spear, *At. Data Nucl. Data Tables* **80**, 35 (2002).
- [39] K. Hagino, N. Takigawa, J. R. Bennett, and D. M. Brink, *Phys. Rev. C* **51**, 3190 (1995).